



RESEARCH LETTER

10.1002/2017GL073578

Key Points:

- Internal stochastic variability-driven hiatus-like decades may occur despite warming of the tropical equatorial Pacific
- Surface temperature patterns may be very different during past and future hiatus decades
- Global ocean heat uptake tends to slow down during hiatus decades

Supporting Information:

- Supporting Information S1

Correspondence to:

T. L. Frölicher,
thomas.froelicher@usys.ethz.ch

Citation:

von Känel L., T. L. Frölicher, and N. Gruber (2017), Hiatus-like decades in the absence of equatorial Pacific cooling and accelerated global ocean heat uptake, *Geophys. Res. Lett.*, *44*, doi:10.1002/2017GL073578.

Received 24 MAR 2017

Accepted 8 JUN 2017

Accepted article online 12 JUN 2017

Hiatus-like decades in the absence of equatorial Pacific cooling and accelerated global ocean heat uptake

Lukas von Känel¹ , Thomas L. Frölicher¹ , and Nicolas Gruber¹ 

¹Environmental Physics, Institute of Biogeochemistry and Pollutant Dynamics, ETH Zürich, Zürich, Switzerland

Abstract A surface cooling pattern in the equatorial Pacific associated with a negative phase of the Interdecadal Pacific Oscillation is the leading hypothesis to explain the smaller rate of global warming during 1998–2012, with these cooler than normal conditions thought to have accelerated the oceanic heat uptake. Here using a 30-member ensemble simulation of a global Earth system model, we show that in 10% of all simulated decades with a global cooling trend, the eastern equatorial Pacific actually warms. This implies that there is a 1 in 10 chance that decadal hiatus periods may occur without the equatorial Pacific being the dominant pacemaker. In addition, the global ocean heat uptake tends to slow down during hiatus decades implying a fundamentally different global climate feedback factor on decadal time scales than on centennial time scales and calling for caution inferring climate sensitivity from decadal-scale variability.

1. Introduction

Between 1998 and 2012 the rate of increase in global mean surface temperature (GMST; 0.15°C/15 years) was only about half of that of the preceding 26 years period [Karl *et al.*, 2015] and much lower than projected by most climate model simulations [Fyfe *et al.*, 2013]. This temporary slowdown in global warming (often called the “global warming hiatus” or “global surface warming slowdown”) occurred despite the unabated and anthropogenically driven increase in radiative forcing. This apparent inconsistency between the observed slowdown in global warming and the continued intensification of radiative forcing and the continued simulated global warming in climate models has generated intense scientific, political, and public debates [Boykoff, 2014], primarily because of its implications for the understanding of the human interference with the climate system.

Several groups of explanations have been proposed to interpret the observed decadal-scale slowdown in global warming. One group of studies suggested that the radiative forcing had increased at a smaller rate in the 2000s than in previous decades [Lean and Rind, 2008; Solomon *et al.*, 2010; Kaufmann *et al.*, 2011; Estrada *et al.*, 2013; Santer *et al.*, 2014]. Other studies suggested that global warming over the last decade had been larger than thought because of previously unaccounted inhomogeneities in the sea surface temperature (SST) data caused by changes in the network of SST observations [Karl *et al.*, 2015] and because of the geographical incompleteness of the observations, especially over the Arctic [Cowtan and Way, 2014]. Although these processes and observational data issues may have affected to some degree recent trends in GMST, the persistent positive planetary energy imbalance at the top of the atmosphere [Trenberth *et al.*, 2014] and the persistent increase in ocean heat storage [Levitus *et al.*, 2012; Roemmich *et al.*, 2015] over the last two decades imply that the recent slowdown in global warming must mainly result from internal stochastic climate variability [e.g., Easterling and Wehner, 2009; Meehl *et al.*, 2011, 2013; Trenberth and Fasullo, 2013; Marotzke and Forster, 2015; Fyfe *et al.*, 2016; Xie *et al.*, 2016; Yan *et al.*, 2016]. Recent research suggests that decadal variability in the Pacific Ocean associated with a persistent negative phase of the Interdecadal Pacific Oscillation (IPO) and the associated increase in subsurface ocean heat uptake due to intensified trade winds is responsible for the recent slowdown in global warming [Meehl *et al.*, 2011; Trenberth and Fasullo, 2013; England *et al.*, 2014; Nieves *et al.*, 2015].

Most climate models that participated in the fifth phase of the Coupled Model Intercomparison Project (CMIP5) simulate an unabated increase in global mean surface temperature since 1998, in contrast to the observed warming slowdown [Fyfe *et al.*, 2013; England *et al.*, 2015]. A small part of the discrepancies may be explained by errors in the volcanic, solar, and greenhouse gas forcing data sets used to drive the CMIP5 models in the 2000s [Schmidt *et al.*, 2014]. However, many studies suggest that the differences are mainly caused by internal stochastic climate variability as the fully coupled models simulate their own magnitude,

frequency, and phasing of internal variability [Maher *et al.*, 2014; Meehl *et al.*, 2014; Marotzke and Forster, 2015; Roberts *et al.*, 2015; Medhaug *et al.*, 2017]. Differences between the models and observations can be reconciled when taking into account internal variability [Maher *et al.*, 2014; Risbey *et al.*, 2014]. Pacemaker experiments that forced the surface of the equatorial Pacific to follow the observed temperature evolution successfully reproduced the recent slowdown in global warming [Kosaka and Xie, 2013], underscoring the dominant role of the tropical Pacific in explaining the recent global temperature evolution. However, recent studies using fully coupled model simulations suggest that a slowdown in global warming may also occur, while the IPO is transitioning into a positive phase [Maher *et al.*, 2014; Roberts *et al.*, 2015] and that other processes in the Indian, Atlantic, and Southern Oceans may also have contributed to the slowdown [Meehl *et al.*, 2013; Dai *et al.*, 2015]. However, these previous studies combined either simulations from a wide range of models with different complexities and with different magnitudes and frequencies of internal variability, or they used simulations with only a small number of ensemble members. Large ensemble simulations with a single climate model have, so far, rarely been used to investigate the probability and mechanisms of global warming hiatus decades [Kay *et al.*, 2015].

Using a global energy budget perspective, several studies concluded that global warming slowdown was accompanied by an accelerated ocean heat uptake during those years [Balmaseda *et al.*, 2013; Drijfhout *et al.*, 2014]. Some studies suggested that the Pacific Ocean had taken up more heat during the recent hiatus period [England *et al.*, 2014], whereas other studies suggest that also the Indian Ocean [Lee *et al.*, 2015], Atlantic Ocean, and Southern Oceans [Chen and Tung, 2014] had contributed to the accelerated global ocean heat uptake. A recent study by Xie *et al.* [2016] questioned the predominant view of an accelerated ocean heat uptake during the hiatus decade. They use climate model simulations to show that ocean heat uptake may actually decrease during hiatus decades, implying distinct energy budgets for natural and anthropogenic changes during decadal hiatus decades. Xie *et al.* [2016] analyzed ocean heat content (OHC) changes in the top 700 m only and thus neglect any potential deep ocean warming [Levitus *et al.*, 2012; Balmaseda *et al.*, 2013; Cheng *et al.*, 2017]. Nevertheless, it has been shown earlier that global OHC changes and GMST are not well correlated on decadal-scale time scales in preindustrial control climate model simulations [Palmer *et al.*, 2011; Palmer and McNeall, 2014]. However, it is difficult to pinpoint the oceanic sink for the “missing heat” [Trenberth *et al.*, 2014; Yan *et al.*, 2016] due to the large historical uncertainty in estimated ocean heat content changes owing to systematic errors in temperature measurements and owing to insufficient temperature data coverage [Cheng *et al.*, 2017]. It remains therefore unclear if the oceanic uptake of heat is accelerated during internal stochastic-driven periods of reduced global warming.

In this paper, we highlight that the equatorial Pacific is not the sole driver for generating hiatus-like decades and we assess ocean heat content changes during hiatus decades. Using output from a 30-member ensemble simulation of a single Earth system model, we show that (i) 10% of the global warming hiatus periods show a warming in the Equatorial Pacific and that (ii) global ocean heat uptake tends to slow down during hiatus periods.

2. Methods

2.1. GFDL ESM2M 30-Member Ensemble Simulation

We use output from a 30-member ensemble simulation [Rodgers *et al.*, 2015] of the global coupled carbon climate Earth system model developed at the Geophysical Fluid Dynamics Laboratory (GFDL ESM2M) [Dunne *et al.*, 2012]. The physical core of the model is based on CM2.1 [Delworth *et al.*, 2006]. The atmospheric model has a horizontal resolution of $2^\circ \times 2.5^\circ$ and 24 vertical levels. The ocean model MOM4p1 consists of 50 vertical levels and has a horizontal resolution of 1° or less.

The individual 30-member ensemble simulations cover the 1950–2100 period and are forced with the same historical and 21st century high business-as-usual greenhouse gas Representative Concentration Pathway 8.5 (RCP8.5) scenario (Figure S1 in the supporting information) [Rodgers *et al.*, 2015]. The individual ensemble members differ only in the initial state of all model components (ocean, land, sea ice, and atmosphere) at midnight of 1 January in year 1950: While ensemble member 1 is a direct continuation of a historical 1861–1949 simulation, the ensemble members 2 to 30 use the state of ensemble member 1 at midnight of 1–29 January in year 1950 as their initial state on 1 January 1950. The state of the El Niño–Southern Oscillation (ENSO) in the ensemble members is randomized within 5 years [Wittenberg *et al.*, 2014]. Thus,

the differences in the initial conditions are sufficient to represent internal stochastic climate variability in the simulation ensemble.

The GFDL ESM2M simulates well the changes in the ocean energy budget over the historical period. The simulated ocean heat uptake since 1960 integrated over different depth levels and the response in ocean heat content to the Pinatubo volcanic eruption is in good agreement with observation-based estimates (Figure S2) [Frölicher *et al.*, 2015; Gleckler *et al.*, 2016].

2.2. Analysis Methods

We focus the identification of hiatus and accelerated warming periods in the large ensemble simulation to the 2005–2024 period. This period has been chosen to minimize the influence of the decadal-scale warming recovery of the Pinatubo eruption in 1991 while still being as close as possible to the observed hiatus period from 1998 to 2014. Observation-based and climate model analysis have shown that the time scale of the GMST recovery after the Pinatubo eruption is about 5–7 years and that the time scale of the OHC recovery, in particular, in the subsurface, is more than a decade (Figure S2c) [Stenchikov *et al.*, 2009; Frölicher *et al.*, 2011; Ding *et al.*, 2014; Lehner *et al.*, 2016]. Hiatus decades are defined as periods with linear decadal GMST trends of zero ($0^{\circ}\text{C decade}^{-1}$) or lower, which contrasts with the decadal 30-member ensemble mean GMST trend between 2005 and 2024 of 0.17°C . To ensure that both the hiatus and accelerated warming decades have the same deviation from the decadal ensemble mean trend, we set the threshold for the accelerated warming decades to $0.34^{\circ}\text{C decade}^{-1}$.

We calculated 330 running linear least squares GMST trends over the 2005–2024 period (30-ensemble members \times 11 decadal trends), and we treated each event independently. If not otherwise stated, surface air temperature and SST are given as a trend anomaly, i.e., the difference between the linear decadal trend during a hiatus or an accelerated warming decade and the ensemble mean trend of the respective decade, the latter reflecting the mean response to the external forcing.

The OHC for different depth levels (0–109 m, 110–788 m, 789–2158 m, and full depth) is determined using the simulated potential ocean temperature T , the simulated sea water potential density ρ , and the specific heat content of sea water c_p : $\text{OHC} = c_p \int_{z_1}^{z_2} T(a, z) \rho(a, z) da dz$. The specific heat capacity of seawater is assumed to be constant ($c_p = 4039.4 \text{ J kg}^{-1} \text{ K}^{-1}$). z_1 and z_2 are the lower and upper limits of the layer depth, and a denotes the surface area. The effect of variations in c_p on OHC is very small and does not affect our main results. The change in OHC is given as the difference between the centered 3 year averages of the first and the last year of the hiatus or accelerated warming decade relative to the ensemble mean change during the same decade. As a measure of the strength of the shallow subtropical overturning cell (STC) we use the difference between the mean meridional overturning circulation (MOC) between 10°N and 20°N and the mean MOC between 20°S and 10°S in the top 150 m of the Pacific. The Indonesian throughflow (ITF) transport is defined as the full depth net transport entering the Indian Ocean at 115°E between 25°S and 8°S . The strength of the Atlantic meridional overturning circulation (AMOC) is calculated as the maximum MOC north of 20°N below 300 m, and the Antarctic Bottom Water (AABW) formation is given by the minimum of the MOC south of 60°S . To remove spurious drifts, all variables analyzed in this study are detrended with a linear trend obtained from an accompanying 150 yearlong preindustrial control integration. The significance of the changes in Figures 2 and 4 are calculated based on an unpaired two-sample t test. The degrees of freedom are approximated using the Welch-Satterthwaite equation and adjusted for autocorrelation.

3. Results

3.1. Simulated Global Mean Surface Temperature Trends

The model simulates 41 hiatus and 41 accelerated warming decades out of the total 330 decadal trends possible within the analysis period and the number of ensemble members (Figure 1a). The probability of simulating hiatus events decreases rapidly for longer trend periods with only three out of one hundred eighty 15 year periods showing a trend lower than zero (Figure 1b). The longest simulated hiatus event lasts 17 years, but we need to point out that the sample size is reduced when analyzing longer hiatus events, as we only analyze the 2005–2024 period. A similar picture emerges for accelerated warming decades (Figure 1c). The 10 year periods with warming larger than $0.34^{\circ}\text{C decade}^{-1}$ are quite common, but there are very few periods

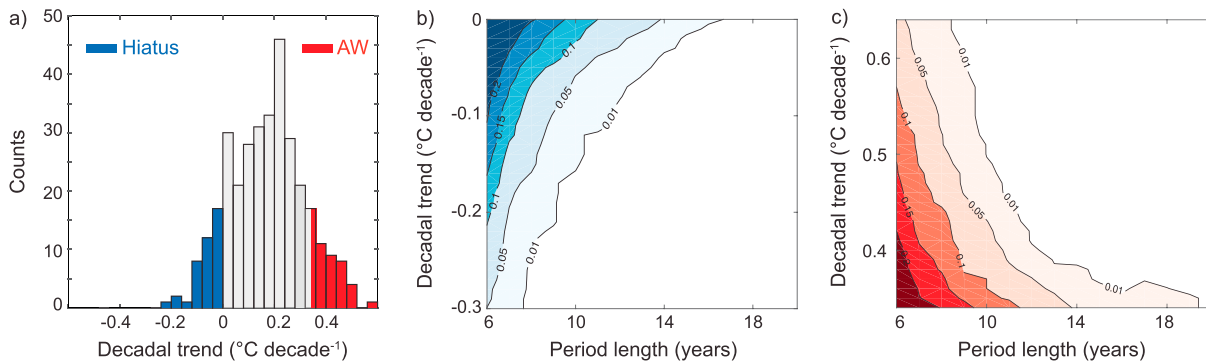


Figure 1. (a) Histogram of 330 simulated decadal GMST trends between 2005 and 2024. Hiatus decades are in blue, and accelerated warming (labeled as “AW”) decades are in red. (b, c) Probability of simulated GMST trends between 2005 and 2024 as a function of trend length (x axis) and trend magnitude (y axis). The largest trend magnitude in Figure 1b and smallest in 1c is the threshold for 1b hiatus ($\leq 0^{\circ}\text{C decade}^{-1}$) and 1c accelerated warming ($\geq 0.34^{\circ}\text{C decade}^{-1}$) decades.

longer than 10 years. The longest simulated accelerated warming period is 19 years. Hiatus and accelerated warming periods are temporally correlated. Following the termination of a hiatus decade, there is a 59% probability of a warmer than average decadal warming trend. Cooling trends become more unlikely in the future under the RCP8.5 greenhouse gas scenario. Only 1 out of 330 decades over the 2041–2060 period is a hiatus decade, and no hiatus decade is simulated over 2081–2100. This is qualitatively in agreement with previous studies [e.g., Easterling and Wehner, 2009; Maher et al., 2014; Roberts et al., 2015; Medhaug and Drange, 2016].

3.2. Simulated Sea Surface Temperature Trend Patterns

A SST trend anomaly composite of the simulated 41 hiatus decades shows cool anomalies in the eastern tropical Pacific, flanked by warm anomalies in the western North Pacific and subtropical South Pacific, reminiscent of a negative IPO phase (Figure 2a). Indeed, the correlation between this anomaly composite pattern and the IPO pattern obtained from a 1500 year preindustrial control simulation of the GFDL ESM2M is relatively high ($r^2 = 0.56$ between $100^{\circ}\text{E}–70^{\circ}\text{W}$ and $40^{\circ}\text{S}–60^{\circ}\text{N}$). The IPO in the control simulation was defined as the second empirical orthogonal function of yearly data smoothed with a 13 year running. The simulated mean SST trend anomaly in the Niño3.4 region is $-0.66^{\circ}\text{C decade}^{-1}$ (blue bars in Figure 2b), larger than the observed trend anomaly of $-0.10^{\circ}\text{C decade}^{-1}$ over 1998–2014 relative 1950–1997 in the Niño3.4 region [Huang et al., 2015]. It has been shown that the GFDL ESM2M simulates rather strong ENSO amplitudes [Bellenger et al., 2014]. During the accelerated warming decades, the ensemble mean SST trend anomaly in the Niño3.4 region is $0.87^{\circ}\text{C decade}^{-1}$ (red bars in Figure 2b). The composite of the SST trend anomaly patterns for the accelerated warming decades is almost exactly opposite to the hiatus composite (Figure S3a). The pattern correlation coefficient (r^2) of the temperature anomaly patterns of the mean hiatus and accelerated warming decades is 0.87.

Whereas the composite of SST trend anomaly patterns during hiatus decades shows a pronounced cooling in the eastern tropical Pacific (Figure 2a), there are four hiatus decades (or 10% of all 41 hiatus decades) that do not simulate a cooling anomaly in the Niño3.4 region (green bars in Figure 2b; Figures 2c–2f). Averaged over the four specific hiatus periods (all cover different time periods but have by definition identical length of 10 years), the simulated SST trend anomaly in the Niño3.4 region is $0.13 \pm 0.08^{\circ}\text{C decade}^{-1}$. Predominant La Niña (or negative IPO) periods thus cannot explain the decadal-scale global cooling in these four specific decades. There are also three accelerated warming decades with negative SST trend anomalies in the Niño3.4 region (brown bars in Figure 2b; Figures S3b–S3d). In addition, decades with strong negative SST trend anomalies in the Niño3.4 region are not necessarily hiatus decades. Only 15 out of 41 hiatus decades are part of the 41 strongest La Niña decades. A similar picture emerges when investigating the IPO instead of the ENSO SST patterns. Strong negative IPO phases are not necessarily hiatus decades. This is because the IPO and ENSO SST patterns in the equatorial Pacific are highly correlated on decadal time scales in GFDL ESM2M.

The individual regional SST trend anomaly patterns of the four specific hiatus periods that simulate warming over the Niño3.4 region are very heterogeneous (Figures 2c–2e; individual SST trend patterns for all 41 hiatus decades are shown in Figure S4). The ratio between the mean of the four-member SST trend anomalies and one standard deviation between the four-member SST trend anomalies is less than 1 in 83% of the ocean

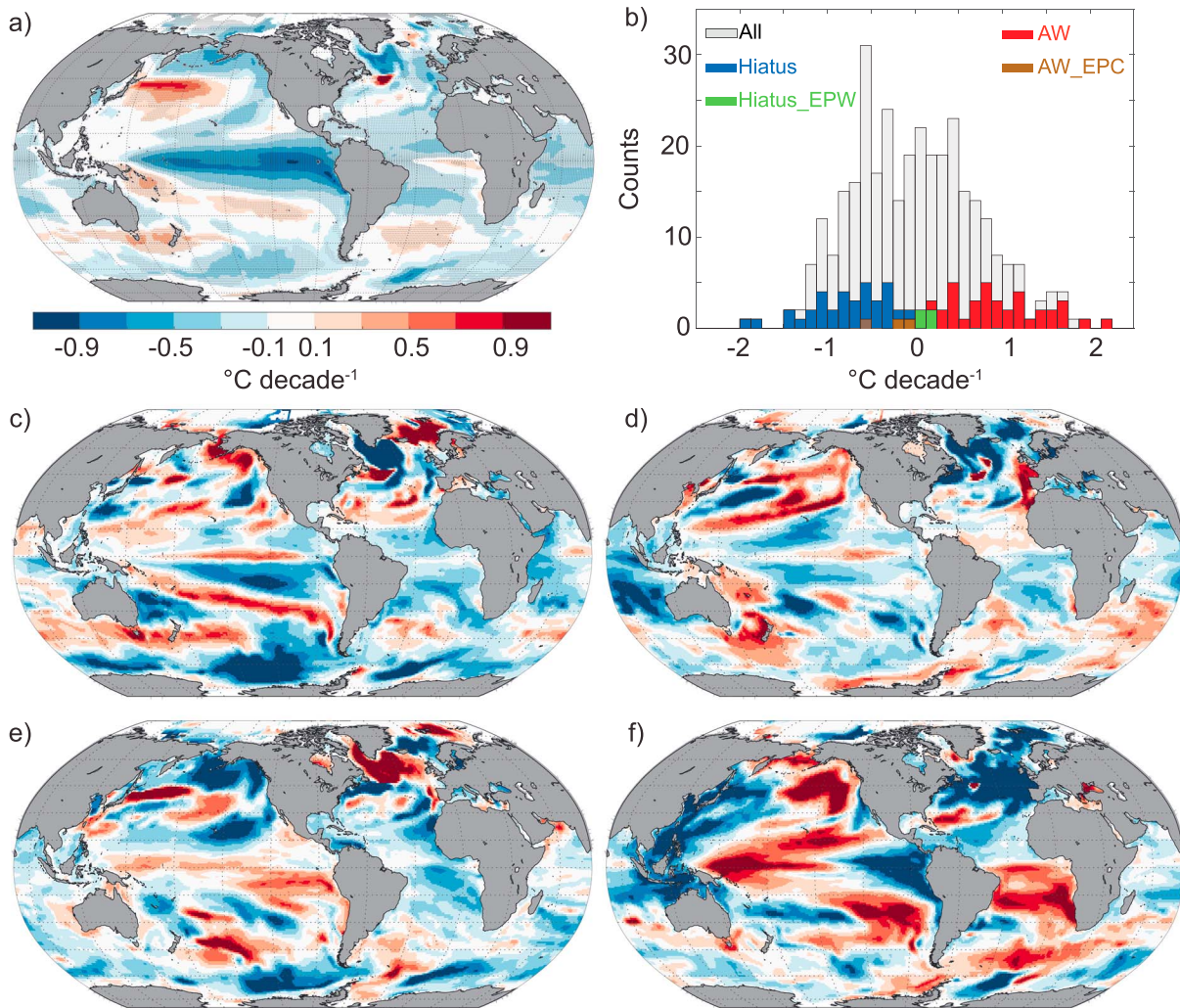


Figure 2. (a) Composite of the simulated SST trend anomaly patterns of all hiatus decades relative to the ensemble mean trend of all ensemble members. (c–f) The same as Figure 2a but for the four individual hiatus decades that have a warming trend anomaly in the Niño3.4 region. (b) SST trend anomalies relative to the ensemble mean in the Niño3.4 region (120°W–170°W, 5°S–5°N) for all individual 330 decades (labeled as “All”; grey), hiatus decades (“Hiatus”, blue), accelerated warming decades (“AW”; red), hiatus decades with a warming trend anomaly in the Niño3.4 region (“Hiatus_EPW,” green), and accelerated warming decades with a cooling trend anomaly (“AW_EPC,” brown). Stippling in Figure 2a indicates significant changes.

surface areas. Using the K-means clustering approach [Arthur and Vassilvitskii, 2007], we could not find any distinctive climate mode or superposition of climate modes that can explain the SST patterns of all these four hiatus decades together.

3.3. Simulated Changes in Ocean Heat Content and Circulation

The rate of change in global OHC is reduced by $0.47 \pm 0.96 \times 10^{22} \text{ J decade}^{-1}$ during hiatus decades (large blue point in Figure 3a) relative to the ensemble mean rate of OHC change of $12.80 \pm 0.97 \times 10^{22} \text{ J decade}^{-1}$. Only 34% of all hiatus decades show a positive anomalous rate of global OHC change during hiatus decades. Only 56% and 29% of all hiatus decades show an increase in the Pacific and Indian Oceans heat content relative to the ensemble mean. However, the spread in OHC changes among the individual hiatus and accelerated warming members is large (individual blue and red points in Figure 3a), implying that SST trends are not characteristic for changes in global OHC and vice versa on decadal time scales (r^2 between decadal OHC changes and decadal SST trends is only 0.21 for all 330 decades). Also, the simulated changes in the anomalous rate of OHC change for the hiatus members with warming in the Niño3.4 region (green crosses in Figure 3a) differ widely. Nonconsistent changes in the rate of OHC changes are also simulated for the accelerated warming decades with cooling in the Niño3.4 region (brown crosses in Figure 3a).

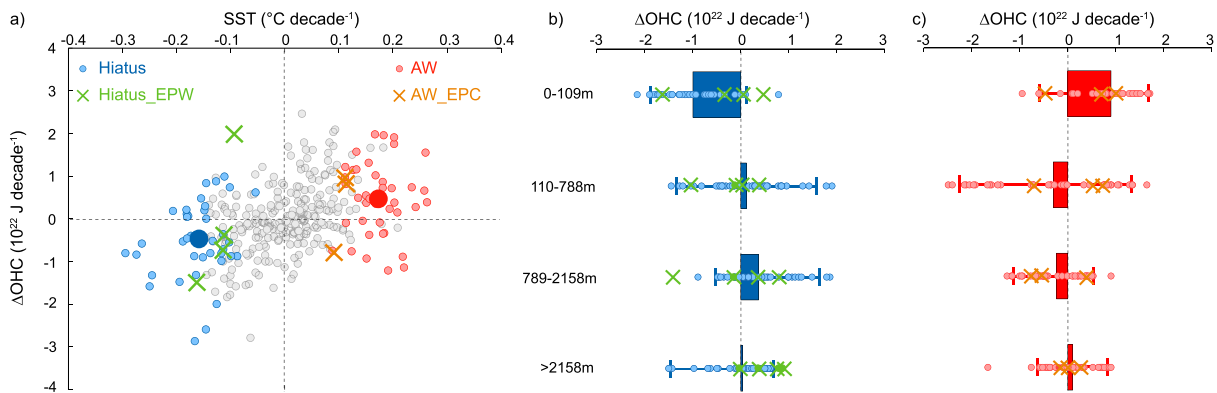


Figure 3. (a) Linear decadal trend in global SST anomalies (x axis) versus decadal changes in the rate of global OHC changes (y axis) relative to the ensemble mean. The large blue and red points indicate the average of all hiatus and accelerated warming decades, respectively. (b) Bars indicate mean changes in the rate of OHC changes during hiatus decades relative to the ensemble mean integrated over different depth levels. (c) The same as Figure 3b but for accelerated warming periods. In all panels, grey points are for all individual decades, light blue points are for hiatus decades, light red points are for accelerated warming decades, green crosses indicate hiatus decades with warming trend anomalies in the Niño3.4 region (Hiatus_EPW), and brown crosses indicate accelerated warming decades with cooling trend anomalies (AW_EPC). The 5th and 95th percentiles are shown with small vertical lines in Figures 3b and 3c.

A large vertical redistribution of ocean heat is simulated during both hiatus (Figure 3b) and accelerated warming decades (Figure 3c). During hiatus decades (Figure 3b), the anomalous rate of OHC changes above 110 m depth is significantly reduced by $1.0 \pm 0.6 \times 10^{22} \text{ J decade}^{-1}$, a reduction of 67% compared to the average trend of all ensemble decades of $1.5 \pm 0.9 \times 10^{22} \text{ J decade}^{-1}$. In deeper layers, the rate of OHC change is enhanced during hiatus decades. Integrated from 110 m to 788 m, the rate of OHC change is $0.12 \pm 0.79 \times 10^{22} \text{ J decade}^{-1}$ larger than the ensemble mean trend of $6.2 \pm 1.0 \times 10^{22} \text{ J decade}^{-1}$. Between 789 and 2158 m, the anomalous rate of OHC changes is $0.37 \pm 0.6 \times 10^{22} \text{ J decade}^{-1}$. Below that, the changes in OHC are small. In general, the spread among the individual hiatus decades is very large and even the sign of the anomalous rate of OHC changes can differ (individual blue points in Figure 3b). The four hiatus decades with warming in the surface equatorial Pacific show all different anomalous rates of OHC changes at the different depth levels (green crosses in Figure 3b). As for SST, the anomalous rates of OHC changes at different depth levels during accelerated warming periods are generally opposite to the hiatus periods (Figure 3c).

A regional breakdown of OHC changes during hiatus decades indicates that 37% of the global decrease in the rate of OHC changes above 110 m occurs in the equatorial Pacific (Figure S5) between 20°N and 20°S (Figure 4a). The stronger STC during hiatus decades ($0.13 \pm 0.66 \text{ Sv}$, Figure 4e) leads to enhanced equatorial upwelling of cold waters to the surface in the eastern equatorial Pacific, reducing the OHC in the upper 100 m (Figures 4a and S6a). At the same time, the stronger STCs enhance the heat convergence in the subtropics of each hemisphere producing warming below 100 m (Figures 4a and S6a). A similar pattern is simulated in the Indian Ocean with a OHC decrease in the top 110 m and an OHC increase in the subsurface of the tropics (Figures 4b and S6b). Part of the tropical subsurface increase stems from local heat reorganizations in the Indian Ocean, but part of the increase also originates from an enhanced heat transport from the Pacific through the Indonesian passages to the Indian Ocean. The ITF strength is not significantly different during hiatus decades than during the ensemble mean ($-0.05 \pm 0.45 \text{ Sv}$, Figure 4f), but the overall heat transport from the Pacific into the Indian Ocean is larger. The reduction in the Atlantic meridional overturning circulation (AMOC) of $0.20 \pm 0.56 \text{ Sv}$ during hiatus decades (Figure 4g) and the associated decrease in the subduction of cold surface water into the deeper ocean causes a warming effect in the subsurface North Atlantic (Figures 4c and S6c). Similarly, the decrease in the AABW of $-0.71 \pm 3.2 \text{ Sv}$ (Figure 4h) and associated reduction in convection of cold surface waters to the deeper ocean causes a small warming south of 60°S at depth during hiatus decades (Figures 4d and S6d). In general, however, the spread in local OHC and ocean circulation changes across the individual hiatus decades is large, and changes are generally not significantly different from ensemble mean changes. This underscores again that no single mechanisms can explain the differences between the hiatus members.

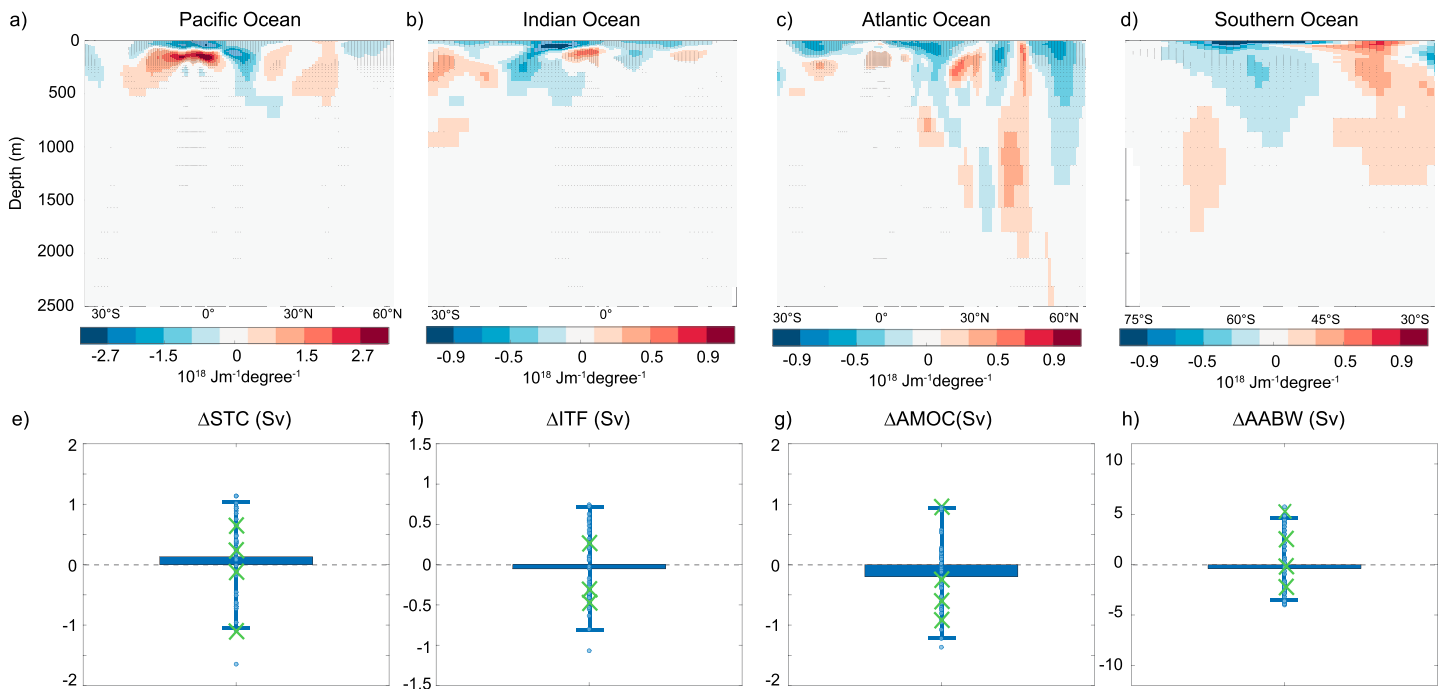


Figure 4. (a–d) Composite of zonally integrated OHC anomalies during hiatus decades relative to the ensemble mean change for the Pacific Ocean (Figure 4a), the Indian Ocean (Figure 4b), the Atlantic Ocean (Figure 4c), and the Southern Ocean (Figure 4d). (e–h) Trend in the strength of the STCs (Figure 4e), the ITF (Figure 4f), the AMOC (Figure 4g), and the AABW (Figure 4h) formation during hiatus decades relative to the ensemble mean trend of all decades. The bars indicate the ensemble mean of all hiatus decades, the points show the individual hiatus decades, and the green crosses indicate the hiatus decades with zero or positive SST trend anomalies in the Niño3.4 region. Stippling in Figures 4a–4d indicates significant changes. The 5th and 95th percentiles are shown with small horizontal lines in Figures 4e–4h.

4. Discussion and Conclusions

We show that the GFDL ESM2M large ensemble simulates a wide range of different anomalous SST trend patterns during hiatus and accelerated warming decades. In general, the dominant driver of causing internal stochastic variability-driven hiatus-like decades is the eastern equatorial tropical Pacific, in agreement with previous studies [Kosaka and Xie, 2013; England et al., 2014]. However, 10% of the simulated hiatus decades are associated with a surface warming of the eastern tropical Pacific implying that there is a 1 in 10 chance that internal stochastic variability-driven hiatus like decades occur without the equatorial Pacific being the dominant pacemaker. Our study agrees with the study by Roberts et al. [2015] who showed that the CMIP5 models can simulate marked differences in the magnitude and patterns of SST changes during hiatus decades. However, the intercomparison of the CMIP5 models is difficult as the models have differing resolutions, physics, and initial conditions. Therefore, the spread in the CMIP5 models usually originates from different model formulations and internal stochastic climate variability. Unlike the CMIP5 model spread, the simulated spread in the anomalous SST trend patterns in our study is based on internal stochastic climate variability alone. Our large 30-member ensemble simulation highlights the large spread in simulated ocean circulation changes and associated changes in OHC and surface warming patterns among the individual ensemble members during hiatus decades. This is in contrast to Meehl et al. [2011, 2013], who use a five-member ensemble simulation to predominately analyze the ensemble mean response.

Simple energy balance models suggest that the surface temperature change is equal the difference between the radiative forcing and the ocean heat uptake divided by the climate feedback parameter [Gregory et al., 2004]. A slowdown in the rate of global warming under constant radiative forcing would therefore imply an accelerated ocean heat uptake. However, our results show that the rate of ocean heat content changes tends to decrease during hiatus periods relative to the ensemble mean, opposite to what is expected from the simple global energy balance model and opposite from what the GFDL ESM2M simulates on centennial time scales [Frölicher et al., 2013]. Xie et al. [2016] have shown that the maximum ocean heat uptake is usually

delayed behind the peak cold phase for interannual-to-decadal variability consistent with our study. Our results imply distinct different relationships between surface temperature and OHC changes for natural decadal-scale variability and long-term anthropogenic warming [Brown *et al.*, 2014; Palmer and McNeill, 2014; Xie *et al.*, 2016]. In other words, the climate feedback factor, which is proportional to OHC changes divided by temperature changes, obtained during decadal-scale hiatus periods may be different and sometimes may even have the opposite sign relative to the climate feedback factor obtained from forced centennial time scale climate change. This calls for caution when inferring long-term feedbacks from short-term observations or model simulations [Dalton and Shell, 2013; Dessler, 2013; Zhou *et al.*, 2016].

We show that the anomalous rate of OHC changes is generally reduced in the top 100 m and enhanced below during hiatus decades, consistent with previous studies [e.g., Meehl *et al.*, 2011]. The enhanced subsurface ocean heat uptake in the Pacific Ocean during hiatus decades is mainly caused by enhanced subduction of heat into the deeper ocean due to stronger subtropical cells in the Pacific Ocean. The anomalous warming in the subsurface tropical Indian Ocean is partly associated with an enhanced heat transport by the ITC. However, the large spread among the individual simulated hiatus decades suggests that no single mechanisms can explain the general increase in subsurface ocean heat uptake [Meehl *et al.*, 2011, 2013; England *et al.*, 2014].

Even though we consider these conclusions as robust, two possible caveats need to be discussed. First, the observed hiatus decade lasted about 15 years (much longer than our 10 year definition of a hiatus period), and the temperature trend over this period was 0.10°C/decade (larger than our decadal SST trend threshold of 0°C/decade). Adopting these threshold, i.e., by defining a hiatus period as a period with a linear 15 year GMST trends of 0.10°C/decade or lower, we identify 36 hiatus periods out of the 210 15 year trends possible between 2005 and 2024 (Figure S7). There are thirteen 15 year periods that do not simulate a cooling anomaly in the Niño3.4 region. Similarly, there are also nine 15 year periods (with a linear 15 year GMST trend of 0.25°C/decade C or higher) that do not simulate a warming anomaly in the Niño3.4 region during an accelerated warming decade. We therefore conclude that our original thresholds, i.e., 10 years with a decadal GMST trend of 0°C or lower, are more stringent to detect hiatus periods. This implies that an internal variability-driven hiatus period with a threshold akin to the observed “hiatus” (with or without warming anomaly in the Niño3.4 region) may occur more often than our analysis suggests. Second, the robustness of our results may depend on the ability of the GFDL ESM2M model to accurately simulate internal stochastic climate variability. Bellenger *et al.* [2014] showed that the GFDL ESM2M model exhibits a broad spectrum of ENSO variability consistent with observations, increasing the confidence in our results. However, the GFDL ESM2M simulates rather strong interannual GMST variations associated with ENSO variability [Dunne *et al.*, 2012; Bellenger *et al.*, 2014]. We tried to account for this bias by using a relative large threshold for the definition of a hiatus decade (i.e., linear decadal GMST trend $\leq 0^\circ\text{C decade}^{-1}$). Nevertheless, our experiments should be repeated with other models, to evaluate the robustness of these results.

In summary, our large ensemble simulations suggest that decadal-scale hiatus periods in global mean surface temperature can arise entirely at random without having colder than normal equatorial Pacific decadal SST trends and accelerated ocean heat uptake. Our results imply limited predictability for decadal forecasts of surface warming and ocean heat content patterns.

Acknowledgments

The authors are grateful to the Geophysical Fluid Dynamics Laboratory model developers for making the GFDL ESM2M available and to Keith Rodgers who was involved in setting up the large ensemble simulations. We thank Iselin Medhaug for comments on the manuscript and Maria Rugenstein for discussions. T.L.F. acknowledges support from the Nippon Foundation-the University of British Columbia Nereus Program. The GFDL ESM2M ensemble data used in this study are available under http://dogfish.princeton.edu/ENSEMBLE_ESM2M/.

References

- Arthur, D., and S. Vassilvitskii (2007), k-means++: The advantages of careful seeding, in *Proceedings of the Eighteenth Annual ACM-SIAM Symposium on Discrete Algorithms*, pp. 1027–1035, Society for Industrial and Applied Mathematics, Philadelphia, Pa.
- Balmaseda, M. A., K. E. Trenberth, and E. Källén (2013), Distinctive climate signals in reanalysis of global ocean heat content, *Geophys. Res. Lett.*, *40*, 1754–1759, doi:10.1002/grl.50382.
- Bellenger, H., E. Guilyardi, J. Leloup, M. Lengaigne, and J. Vialard (2014), ENSO representation in climate models: From CMIP3 to CMIP5, *Clim. Dyn.*, *42*(7–8), 1999–2018, doi:10.1007/s00382-013-1783-z.
- Boykoff, M. T. (2014), Media discourse on the climate slowdown, *Nat. Clim. Change*, *4*(3), 156–158, doi:10.1038/nclimate2156.
- Brown, P. T., W. Li, L. Li, and Y. Ming (2014), Top-of-atmosphere radiative contribution to unforced decadal global temperature variability in climate models, *Geophys. Res. Lett.*, *41*, 5175–5183, doi:10.1002/2014GL060625.
- Chen, X., and K.-K. Tung (2014), Varying planetary heat sink led to global-warming slowdown and acceleration, *Science*, *345*(6199), 897–903, doi:10.1126/science.1254937.
- Cheng, L., K. E. Trenberth, J. Fasullo, T. Boyer, J. Abraham, and J. Zhu (2017), Improved estimates of ocean heat content from 1960 to 2015, *Sci. Adv.*, *3*, 1–11, doi:10.1126/sciadv.1601545.
- Cowtan, K., and R. G. Way (2014), Coverage bias in the HadCRUT4 temperature series and its impact on recent temperature trends, *Q. J. R. Meteorol. Soc.*, *140*(683), 1935–1944, doi:10.1002/qj.2297.

- Dai, A., J. C. Fyfe, S.-P. Xie, and X. Dai (2015), Decadal modulation of global surface temperature by internal climate variability, *Nat. Clim. Change*, 5(6), 555–559, doi:10.1038/nclimate2605.
- Dalton, M. M., and K. M. Shell (2013), Comparison of short-term and long-term radiative feedbacks and variability in twentieth-century global climate model simulations, *J. Clim.*, 26(24), 10,051–10,070, doi:10.1175/JCLI-D-12-00564.1.
- Delworth, T. L., et al. (2006), GFDL's CM2 global coupled climate models. Part I: Formulation and simulation characteristics, *J. Clim.*, 19(5), 643–674, doi:10.1175/JCLI3629.1.
- Dessler, A. E. (2013), Observations of climate feedbacks over 2000–10 and comparisons to climate models, *J. Clim.*, 26(1), 333–342, doi:10.1175/JCLI-D-11-00640.1.
- Ding, Y., J. Carton, G. A. Chepurin, G. Stenchikov, A. Robock, L. T. Sentman, and J. P. Krasting (2014), Ocean response to volcanic eruptions in Coupled Model Intercomparison Project 5 simulations, *J. Geophys. Res. Atmos.*, 119, 5622–5637, doi:10.1002/2013JC009780.
- Drijfhout, S. S., A. T. Blaker, S. A. Josey, A. J. G. Nurser, B. Sinha, and M. A. Balmaseda (2014), Surface warming hiatus caused by increased heat uptake across multiple ocean basins, *Geophys. Res. Lett.*, 41, 7868–7874, doi:10.1002/2014GL061456.1.
- Dunne, J. P., et al. (2012), GFDL's ESM2 global coupled climate-carbon Earth system models. Part I: Physical formulation and baseline simulation characteristics, *J. Clim.*, 25, 6646–6665, doi:10.1175/JCLI-D-11-00560.1.
- Easterling, D. R., and M. F. Wehner (2009), Is the climate warming or cooling?, *Geophys. Res. Lett.*, 36, L08706, doi:10.1029/2009GL037810.
- England, M. H., S. McGregor, P. Spence, G. A. Meehl, A. Timmermann, W. Cai, A. Sen Gupta, M. J. McPhaden, A. Purich, and A. Santoso (2014), Recent intensification of wind-driven circulation in the Pacific and the ongoing warming hiatus, *Nat. Clim. Change*, 4(3), 222–227, doi:10.1038/NCLIMATE2106.
- England, M. H., J. B. Kajtar, and N. Maher (2015), Robust warming projections despite the recent hiatus, *Nat. Clim. Change*, 5(5), 394–396, doi:10.1038/nclimate2575.
- Estrada, F., P. Perron, and B. Martínez-López (2013), Statistically derived contributions of diverse human influences to twentieth-century temperature changes, *Nat. Geosci.*, 6(12), 1050–1055, doi:10.1038/ngeo1999.
- Frölicher, T. L., F. Joos, and C. C. Raible (2011), Sensitivity of atmospheric CO₂ and climate to explosive volcanic eruptions, *Biogeosciences*, 8(8), 2317–2339, doi:10.5194/bg-8-2317-2011.
- Frölicher, T. L., M. Winton, and J. L. Sarmiento (2013), Continued global warming after CO₂ emissions stoppage, *Nat. Clim. Change*, 4(1), 40–44, doi:10.1038/nclimate2060.
- Frölicher, T. L., J. L. Sarmiento, D. J. Paynter, J. P. Dunne, J. P. Krasting, and M. Winton (2015), Dominance of the Southern Ocean in anthropogenic carbon and heat uptake in CMIP5 models, *J. Clim.*, 28(2), 862–886, doi:10.1175/JCLI-D-14-00117.1.
- Fyfe, J. C., N. P. Gillett, and F. W. Zwiers (2013), Overestimated global warming over the past 20 years, *Nat. Clim. Change*, 3(9), 767–769, doi:10.1038/nclimate1972.
- Fyfe, J. C., et al. (2016), Making sense of the early-2000s warming slowdown, *Nat. Clim. Change*, 6(3), 224–228, doi:10.1038/nclimate2938.
- Gleckler, P. J., P. J. Durack, R. J. Stouffer, G. C. Johnson, and C. E. Forest (2016), Industrial-era global ocean heat uptake doubles in recent decades, *Nat. Clim. Change*, 6(4), 394–398, doi:10.1038/nclimate2915.
- Gregory, J. M., W. J. Ingram, M. A. Palmer, G. S. Jones, P. A. Stott, R. B. Thorpe, J. A. Lowe, T. C. Johns, and K. D. Williams (2004), A new method for diagnosing radiative forcing and climate sensitivity, *Geophys. Res. Lett.*, 31, L03205, doi:10.1029/2003GL018747.
- Huang, B., V. F. Banzon, E. Freeman, J. Lawrimore, W. Liu, T. C. Peterson, T. M. Smith, P. W. Thorne, S. D. Woodruff, and H. M. Zhang (2015), Extended reconstructed sea surface temperature version 4 (ERSST.v4). Part I: Upgrades and intercomparisons, *J. Clim.*, 28(3), 911–930, doi:10.1175/JCLI-D-14-00006.1.
- Karl, T. R., A. Arguez, B. Huang, J. H. Lawrimore, J. R. McMahon, M. J. Menne, T. C. Peterson, R. S. Vose, and H.-M. Zhang (2015), Possible artifacts of data biases in the recent global surface warming hiatus, *Science*, 348(6242), 1469–1472, doi:10.1126/science.aaa5632.
- Kaufmann, R. K., H. Kauppi, M. L. Mann, and J. H. Stock (2011), Reconciling anthropogenic climate change with observed temperature 1998–2008, *Proc. Natl. Acad. Sci. U.S.A.*, 108(29), 11,790–11,793, doi:10.1073/pnas.1102467108.
- Kay, J. E., et al. (2015), The community earth system model (CESM) large ensemble project: A community resource for studying climate change in the presence of internal climate variability, *Bull. Am. Meteorol. Soc.*, 96(8), 1333–1349, doi:10.1175/BAMS-D-13-00255.1.
- Kosaka, Y., and S.-P. Xie (2013), Recent global-warming hiatus tied to equatorial Pacific surface cooling, *Nature*, 501(7467), 403–407, doi:10.1038/nature12534.
- Lean, J. L., and D. H. Rind (2008), How natural and anthropogenic influences alter global and regional surface temperatures: 1889 to 2006, *Geophys. Res. Lett.*, 35, L18701, doi:10.1029/2008GL034864.
- Lee, S.-K., W. Park, M. O. Baringer, A. L. Gordon, B. Huber, and Y. Liu (2015), Pacific origin of the abrupt increase in Indian Ocean heat content during the warming hiatus, *Nat. Geosci.*, 8, 445–449, doi:10.1038/ngeo2438.
- Lehner, F., A. P. Schurer, G. C. Hegerl, C. Deser, and T. L. Frölicher (2016), The importance of ENSO phase during volcanic eruptions for detection and attribution, *Geophys. Res. Lett.*, 43, 2851–2858, doi:10.1002/2016GL067935.
- Levitus, S., et al. (2012), World ocean heat content and thermosteric sea level change (0–2000 m), 1955–2010, *Geophys. Res. Lett.*, 39, L10603, doi:10.1029/2012GL051106.
- Maher, N., A. Sen Gupta, and M. H. England (2014), Drivers of decadal hiatus periods in the 20th and 21st centuries, *Geophys. Res. Lett.*, 41, 5978–5986, doi:10.1002/2014GL060527.
- Marotzke, J., and P. M. Forster (2015), Forcing, feedback and internal variability in global temperature trends, *Nature*, 517(7536), 565–570, doi:10.1038/nature14117.
- Medhaug, I., and H. Drange (2016), Global and regional surface cooling in a warming climate: A multi-model analysis, *Clim. Dyn.*, 46(11), 3899–3920, doi:10.1007/s00382-015-2811-y.
- Medhaug, I., M. B. Stolpe, E. M. Fischer, and R. Knutti (2017), Reconciling controversies about the “global warming hiatus”, *Nature*, 545(7652), 41–47, doi:10.1038/nature22315.
- Meehl, G. A., J. M. Arblaster, J. T. Fasullo, A. Hu, and K. E. Trenberth (2011), Model-based evidence of deep-ocean heat uptake during surface-temperature hiatus periods, *Nat. Clim. Change*, 1(7), 360–364, doi:10.1038/nclimate1229.
- Meehl, G. A., A. Hu, J. M. Arblaster, J. Fasullo, and K. E. Trenberth (2013), Externally forced and internally generated decadal climate variability associated with the interdecadal pacific oscillation, *J. Clim.*, 26(18), 7298–7310, doi:10.1175/JCLI-D-12-00548.1.
- Meehl, G. A., H. Teng, and J. M. Arblaster (2014), Climate model simulations of the observed early-2000s hiatus of global warming, *Nat. Clim. Change*, 4(10), 898–902, doi:10.1038/nclimate2357.
- Nieves, V., J. K. Willis, and W. C. Patzert (2015), Recent hiatus caused by decadal shift in Indo-Pacific heating, *Science*, 349(6247), 532–535, doi:10.1126/science.aaa4521.
- Palmer, M. D. and D. J. McNeill (2014), Internal variability of Earth's energy budget simulated by CMIP5 climate models, *Environ. Res. Lett.*, 9(3), 34016, doi:10.1088/1748-9326/9/3/034016.

- Palmer, M. D., D. J. McNeall, and N. J. Dunstone (2011), Importance of the deep ocean for estimating decadal changes in Earth's radiation balance, *Geophys. Res. Lett.*, *38*, L13707, doi:10.1029/2011GL047835.
- Risbey, J. S., S. Lewandowsky, C. Langlais, D. P. Monselesan, T. J. O. Kane, and N. Oreskes (2014), Well-estimated global surface warming in climate projections selected for ENSO phase, *Nat. Clim. Change*, *4*, 835–840, doi:10.1038/NCLIMATE2310.
- Roberts, C. D., M. D. Palmer, D. McNeall, and M. Collins (2015), Quantifying the likelihood of a continued hiatus in global warming, *Nat. Clim. Change*, *5*, 1–6, doi:10.1038/nclimate2531.
- Rodgers, K. B., J. Lin, and T. L. Frölicher (2015), Emergence of multiple ocean ecosystem drivers in a large ensemble suite with an Earth system model, *Biogeosciences*, *12*(11), 3301–3320, doi:10.5194/bg-12-3301-2015.
- Roemmich, D., J. Church, J. Gilson, D. Monselesan, P. Sutton, and S. Wijffels (2015), Unabated planetary warming and its ocean structure since 2006, *Nat. Clim. Change*, *5*(3), 240–245, doi:10.1038/nclimate2513.
- Santer, B. D., et al. (2014), Volcanic contribution to decadal changes in tropospheric temperature, *Nat. Geosci.*, *7*(3), 185–189, doi:10.1038/NCEO2098.
- Schmidt, G. A., D. T. Shindell, and K. Tsigaridis (2014), Reconciling warming trends, *Nat. Geosci.*, *7*(3), 158–160, doi:10.1038/ngeo2105.
- Solomon, S., K. H. Rosenlof, R. W. Portmann, J. S. Daniel, S. M. Davis, T. J. Sanford, and G.-K. Plattner (2010), Contributions of stratospheric water vapor to decadal changes in the rate of global warming, *Science*, *327*(5970), 1219–1223, doi:10.1126/science.1182488.
- Stenchikov, G., T. L. Delworth, V. Ramaswamy, R. J. Stouffer, A. Wittenberg, and F. Zeng (2009), Volcanic signals in oceans, *J. Geophys. Res.*, *114*, D16104, doi:10.1029/2008JD011673.
- Trenberth, K. E., and J. T. Fasullo (2013), An apparent hiatus in global warming?, *Earth's Future*, *1*(1), 19–32, doi:10.1002/2013EF000165.
- Trenberth, K. E., J. T. Fasullo, and M. A. Balmaseda (2014), Earth's energy imbalance, *J. Clim.*, *27*, 3129–3144, doi:10.1175/JCLI-D-13-00294.1.
- Wittenberg, A. T., A. Rosati, T. L. Delworth, G. A. Vecchi, and F. Zeng (2014), ENSO modulation: Is it decadal predictability?, *J. Clim.*, *27*(7), 2667–2681, doi:10.1175/JCLI-D-13-00577.1.
- Xie, S.-P., Y. Kosaka, and Y. M. Okumura (2016), Distinct energy budgets for anthropogenic and natural changes during global warming hiatus, *Nat. Geosci.*, *9*, 29–33, doi:10.1038/ngeo2581.
- Yan, X., T. Boyer, K. Trenberth, T. R. Karl, S. Xie, V. Nieves, K. Tung, and D. Roemmich (2016), The global warming hiatus: Slowdown or redistribution?, *Earth's Future*, *4*, 472–482, doi:10.1002/2016EF000417.
- Zhou, C., M. D. Zelinka, and S. A. Klein (2016), Impact of decadal cloud variations on the Earth's energy budget, *Nat. Geosci.*, *9*(12), 871–874, doi:10.1038/ngeo2828.